Wafer-Scale Laser Pantography: VI. Direct-Write Interconnection Of VLSI Gate Arrays

McWilliams, Bruce, Chin, Hon, Herman, Irving, Hyde, Roderick, Mitlitsky, Fred, et al.

Bruce M McWilliams, Hon Wah Chin, Irving P Herman, Roderick A. Hyde, Fred Mitlitsky, John C. Whitehead, Lowell L. Wood, "Wafer-Scale Laser Pantography: VI. Direct-Write Interconnection Of VLSI Gate Arrays," Proc. SPIE 0459, Laser-Assisted Deposition, Etching, and Doping, (14 June 1984); doi: 10.1117/12.939434

Event: 1984 Los Angeles Technical Symposium, 1984, Los Angeles, United States

Wafer-Scale Laser Pantography: VI. Direct-Write Interconnection of VLSI Gate Arrays

Bruce M. McWilliams, Hon Wah Chin, Irving P. Herman, Roderick A. Hyde
Fred Mitlitsky, John C. Whitehead and Lowell L. Wood

Special Studies Program
University of California
Lawrence Livermore National Laboratory
P.O. Box 808, L-278, Livermore, CA 94550

Abstract

General principles of laser direct-write deposition processes are reviewed. Device interconnection of CMOS gate arrays by means of computer-controlled, laser-induced thermochemical surface reactions is described. Interconnection quality parameters are related, and processing rate considerations are discussed.

Introduction

Interconnection of high performance active devices on semiconductor substrates is recognized as one of the pacing items in extending the limits of integrated circuitry. Indeed, as the ultra-large scale integration (ULSI) plateau is approached, the reliable creation of adequately low resistance and sufficiently dense interconnections between transistors may dominate the formation of the devices themselves as the crucial technology. In addition, the comparative immutability of integrated circuitry places a high premium on the ability to rapidly implement a VLSI/ULSI design, in support of design iteration activity.

We describe here the application of a direct-write technique for discretionally interconnecting at high speed the active elements of a VLSI integrated circuit substrate. In both the work reported here and similar endeavors still underway, we employ gate arrays as model systems for direct-write interconnection R&D; the present work employs CMOS gate arrays with 5000 devices per unit.

Our direct-write approach uses the focused, switched beam from a CW argon ion laser to similarly switch thermochemical reactions between the gate array surface and an overlying atmosphere. The composition and pressure of the gas mixture are chosen to produce chemical reactions of the desired kind and degree in the time interval of interest. In the present case, this reaction is the deposition (on a thin silicon dioxide layer overlying a silicon substrate) of a metal (e.g., tungsten), a metal silicide (e.g., tungsten silicide), or polysilicon sufficiently heavily doped to have adequately high conductivity.

Chemical Reactions For Laser Deposition

A variety of laser-induced interconnection formation processes have been studied.[1-10] These fall into two broad classes: photolytic and pyrolytic processes. The photolytic processes are based on local laser-induced photodecomposition reactions occurring either at the substrate and/or in the gas phase. The pyrolytic processes are based on chemical vapor deposition reactions which occur due to local heating from a focused laser beam incident on the substrate. In applications for IC manufacture, pyrolytic processes have the advantages of exhibiting generally substantially higher rates with presently available laser technology and, since they are based on chemical reactions already used in IC manufacture, they interface more readily with typical IC processes and materials.

There are two basic groups of laser-driven pyrolytic processes which might be applied to interconnection of device structures in integrated circuits. One group is the surface-catalyzed unimolecular thermodecomposition reactions, such as those involving carbonyls[3,5,6] and silanes[7-9]. Two examples of particular interest are

$$Ni(CO)_4 \rightarrow Ni(s) + 4CO \quad (1)$$

$$SiH_4 \rightarrow Si(s) + 2H_2 \quad (2)$$

These reactions are based on reactants which at room temperature have vapor pressures of at least a few hundred Torr and deposit materials which have high melting points, thus potentially allowing relatively fast deposition rates (as explained below). The other groups of reactions are "bimolecular" reactions, typically involving reduction of metal halides. Two reactions of this type which are useful for deposition of tungsten microstructures are [4,10]

$$WF_6 + 3H_2 \rightarrow W(s) + 6HF \quad (3)$$

$$WF_6 + \frac{3}{2}Si(s) \rightarrow W(s) + \frac{3}{2}SiF_4 \quad (4)$$

Since tungsten and tungsten silicide are quite promising interconnect materials for next-generation VLSI/ULSI circuitry, direct-write laser processes which rapidly generate high quality W and WSi_2 interconnections could be very useful.

Tungsten deposition by silicon reduction of tungsten hexafluoride (reaction 4) offers the interesting possibility of being used as a bulk process following direct-write of a silicon interconnect structure by a laser process based on reaction (2). This approach greatly increases the conductivity of the laser-patterned polysilicon structure at the cost of only a small amount of processing time. Furthermore, it produces a more stable structure than direct deposition of tungsten by reaction (3), since the silicon acts as a passivation and adhesion enhancement layer between the oxide and tungsten.

An inherent advantage of direct-write laser processes is their sequential nature which allows on-line changes of the interconnect structures for circumventing defects in devices or interconnect structures. In general, such changes can require both etching and deposition processes. For removal of silicon and various metal structures, processes based on halogen containing gases have been studied and reported.[11-13]

Reaction Kinetics For Laser Deposition

Since laser-induced deposition processes proceed in a sequential manner, one of the most important issues to be considered is reaction kinetics.

Laser-induced pyroltyic deposition processes can be thought of as involving five consecutive steps:

1. Transport of the reactant gas to the laser-heated portion of the substrate;
2. Adsorption of the reactant on the substrate surface;
3. Decomposition of the reactant gas on the heated portion of the surface;
4. Desorption of the volatile product from the heated surface; and
5. Transport of the product gas away from the substrate surface.

The rate-limiting factors of such processes are generally either set by the chemical reaction rate (steps 2, 3 and 4) or are due to gas transport effects (steps 1 and 5).

The temperature- and pressure-dependence of the chemical reaction rate after the nucleation phase of the process is described by an Arrhenius-type relation of the form:

$$R = R_o e^{-T_A/T} P^n \tag{5}$$

where P is the reactant gas pressure, T is the substrate temperature, n is the reaction order and T_A is the activation temperature.

At low temperatures, the deposition rates are limited by the surface reaction rate of Eq. 5. Clearly, this process can be accelerated by increasing the incident laser power, and hence the surface temperature. As this is done, the surface reaction rate eventually outstrips the ability of the gas to deliver reactants and/or to remove reaction products. As a result the deposition rate does not continue to climb with laser power, but eventually saturates.

A general treatment of the transport of reactant and product gases during laser deposition is difficult. The character of the transport depends critically on two parameters: whether the reaction absorbs or liberates gas molecules; and the ratio of the hot spot size, ρ, to the molecular mean-free path, Λ.

If the Knudsen number, $Kn = \Lambda/\rho$, is very large, then the effects of gas transport are easily calculated. In this molecular flow regime, reactant species are supplied to the surface at a rate of

$$F_i = \frac{1}{4} n_i \bar{v}_i \tag{6}$$

where F_i is the number of molecules per second per area striking the surface, $\bar{v}_i$ is the average molecular speed of reactant species i, and n_i' is its molecular density. In this flow regime, the ejected molecules free-stream away from the hot spot, creating a local atmosphere of reaction products. However, because the ejection speeds are greater than those of reactant gases and are more effectively directed, these product densities are low, and should not choke the reaction. Hence, in the molecular flow regime, the deposition rate saturates at a level dictated by the slowest influx rate. For Si deposition by silane, this rate is $\approx 75\ \mu m\ sec^{-1}\ Torr^{-1}$.

While the molecular flow regime is easy to analyze, it can only be assumed for large Knudsen numbers, which for micron-scale spots implies pressures below about 10 Torr. Since we generally operate at higher gas densities in order to increase the deposition rate, the actual molecular flow is strongly influenced by gas collisions.

Accurate calculation of the gas transport in the fluid regime is difficult, involving both diffusion and convection of multiple species. The analysis is even more complicated in the $p \approx$ 100 Torr regime, in which transport is in transition between the molecular and fluid regimes. Accordingly, we will only qualitatively discuss transport at such gas densities.

The flow will strongly depend upon the reaction balance of gas molecules. If the reaction absorbs more gas molecules than are liberated, then reactants can be supplied to the hot spot at sonic velocities. The specific influx rate ranges from the molecular limit of Eq. 6, to a rate about 70% higher in the fluid limit. If there are no product gases, the gas transport rate can then be monotonically increased by raising the gas density, until the surface rate of Eq. 5 is reached. Product gases will have to diffuse away from the hot spot against the reactant influx, and if present can thus choke off the reaction.

However most reactions, including the ones discussed earlier, liberate at least as many molecules as they absorb. In the case where there is no net molecular generation, then the gas convection is relatively weak. Here the transport of reactants and products is a diffusion limited process. This case was analyzed for constant gas diffusion constants in[3]. The specific transport rates scale as D/ρ, a considerably lower velocity than the sonic rate. Furthermore, one cannot arbitrarily increase the deposition rate by increasing gas density. Once the reactant density dominates the total density, then the diffusion coefficient will decrease, and the transport limited deposition rate will saturate.

The general case involves some outward convection, because most reactions liberate more molecules than they absorb and because the gas is emitted at high speed. This means that deposition is limited more by the supply of reactants than by removal of products. The diffusion velocity will then be an upper bound on the specific influx rate, since incoming gas must travel against an outward convection. However, while this convection will slow the influx rate, it will not completely dominate the flow, since the emission of gas depends on the influx-limited reaction rate.

The accurate calculation of gas transport limited deposition rates will probably require a Monte-Carlo analysis. In the absence of such precise results, we expect gas limited deposition rates to saturate in the neighborhood of 1 cm sec^{-1}, for 1 micron-scale traces.

Laser Beam-Substrate Interactions

The temperature field produced during a typical laser deposition process is dependent on substrate features such as the field insulation thickness overlaying device structures, and by the shape and composition of material being deposited. Since this is quite difficult to model, it is usually easier to determine experimentally the correct laser intensity profiles for the desired deposition patterns. However, for making first-order estimates on laser requirements, it is useful to review the analytic solution for a scanning Gaussian profile beam incident on a plain slab of silicon.

The temperature field produced in a plain slab of solid silicon by a linearly swept laser beam of Gaussian profile has been treated previously.[3,14,15] Using a Kirchhoff transform we define a linearized temperature:

$$\theta(T) = \int_{T_r}^{T} \frac{K(T')}{K(T_r)} dT' \tag{7}$$

where T_r is the reference (initial) temperature. Writing the space- and time-dependent laser intensity I as

$$I(x-vt,y)=\frac{P}{\pi r_0^2}\exp\left\{-\frac{(x-vt)^2+y^2}{r_0^2}\right\} \tag{8}$$

where P is the incident laser power and v is the laser focal spot sweep rate, then

$$\theta(X,Y,Z;V)=\frac{2}{\pi}\theta_e\int_0^\infty \exp\left\{-\frac{(X+Vu^2)^2+Y^2}{1+u^2}-\frac{Z^2}{u^2}\right\}\frac{du}{1+u^2} \tag{9}$$

where

$$X=\frac{x}{r_0}\qquad Y=\frac{y}{r_0}\qquad Z=\frac{z}{r_0}\qquad V=\frac{vr_0}{\sqrt{8D}} \tag{10}$$

$$\theta_e=\frac{P(1-\Re_S)}{2\sqrt{\pi}K(T_r)r_0} \tag{11}$$

where θ_e is the peak value of the linearized temperature for the static case, $\Re_S$ is the surface reflectivity, $K(T_r)$ is the substrate thermal conductivity at room temperature, and r_o is the laser beam radius (1/e intensity).

The Green's function technique used in this derivation is not strictly permitted, since the thermal diffusivity has an implicit space and time dependence via its explicit thermal dependence. However, for "relatively slow" scan velocities, D is of little importance as we are in the steady-state limit. We can then convert the linearized temperature θ_e to an absolute value. For silicon, this leads to the relation

$$T_e=99+201\exp\left\{\frac{P(1-\Re_S)/r_o}{1060}\right\} \tag{12}$$

Surface reaction rates, as in Eq. 5, are exponentially sensitive to temperature. This results in an effective hot spot radius ρ which is typically about 40% the size of the actual laser spot r_0.

When depositing foreign material on a substrate, the thermal calculation becomes much more complex. For example, when a metal layer is deposited onto a Si or SiO_2 substrate, lateral conduction along the layer will be stronger than that down into the substrate. Green's function calculations of layered structures[16] are correct only if properties are independent of temperature, or for the steady state case if thermal conductivities of the layers have the same temperature dependence. The general problem, particularly when the upper layer is of limited spatial extent, must be solved numerically.

Experimental Procedure

The laser microscope used in this study permitted simultaneous laser irradiation and viewing of the gate array, as depicted in Figure 1. As detailed in previous descriptions of this experimental apparatus[3,9], laser pulses are formed by electro-optic modulation of the output of a CW argon-ion laser oscillating at 5145 Å. The x-y motion of the wafer-containing reaction vessel is coordinated with the laser pulses by computer control.

The aluminum overcoating on the vendor-supplied gate arrays was removed and the dies were cleaned, both by conventional wet processing. After insertion of the gate arrays, the reaction chamber was baked out under vacuum. Various mixtures of phosphine and silanes or tungsten hexafluoride and hydrogen were then introduced into the cell for doped polysilicon or tungsten deposition, respectively.

After the initial preparation of a gate array, as described above, the chip surface consisted of a roughly 1μm thick silicon dioxide insulation layer overlaying the entire die except for via holes to underlying polysilicon areas of transistor gate/source/-drain regions or polysilicon interconnects. Various structures were fabricated on these gate arrays using direct laser-writing in order to study the deposit morphology, bulk electrical resistance, punch through to the underlying structure, and contact resistance in connections through the vias to the gate array features. Individual transistors were wired to laser-deposited pads and tested by electrical probing.

Results and Analysis

In one group of experiments, reaction (2) was examined. The following results were obtained using an 825 Torr silane mixture laced with 0.1% PH_3 for doping. The substrate was translated relative to the fixed laser beam which was switched on for 50-200 μsec per 0.1 μm of wafer travel to deposit polysilicon interconnecting lines. The focusing objective lens was sufficiently defocused so that the deposition width was as wide as the 5 μm diameter via holes. The deposition of low resistivity material and the successful connection to gate array structures was demonstrated in this experiment.

Electrical resistance of laser deposited polysilicon lines was measured by the four-point probe technique. Five polysilicon lines with an average length of 2.5 mm were deposited on the gate array insulating oxides (see figure 3). Laser-deposited probe pads connected at 250 μm intervals to each line provided resistance data on a total of 32 segments of this length. The resistance data was coupled with a single profilometry trace across each line segment which was integrated to determine cross-sectional area, to obtain the doped polysilicon resistivity. The deposited traces were typically 3-5 μm wide by 1 μm thick as shown by profilometry, and the uniformity of the microstructure cross-sections was confirmed by scanning electron micrographs.

For the 28 line segments used in this measurement, the average resistivity was 3.5×10^{-3} ohm-cm with the best measurements below 3×10^{-3} ohm-cm. (For reasons discussed below, four segments were not included in this analysis.) This resistivity is approximately an order of magnitude lower than that measured for our earlier deposits,[4] and is probably due to improved deposit morphology. The silicon resistivity of 3.5×10^{-3} ohm-cm (~ 35 ohms/square) is about as low as for polysilicon deposited by conventional vapor deposition methods.[17-19] The resistance between two adjacent written lines was measured to be greater than 10^{10} ohms, demonstrating good isolation between individual laser deposits and suggesting minimal thermal damage to the underlying silicon dioxide layer.

In only four of these 250 μm long segments were the measured resistance values abnormally above average. Scanning electron microscopy examination revealed rare morphology defects due to poor step coverage in regions of underlying polysilicon interconnects (and thus ~ 1 μm high oxide steps) running perpendicular to the deposited lines. These defects occurred rarely and their cause is currently under examination. In these early studies, such morphology defects were observed in only one in 1500 traversed steps. This suggests that they are not an inherent problem of this process.

Some deposited line segments on the same gate array were diverted through the underlying polysilicon interconnects. Electrical continuity was verified through these traces, thus demonstrating the compatibility of this process with the use of polysilicon tunnels to expedite routing.

The one remaining requirement necessary to wire gate array circuits by laser writing is the demonstrated electrical hookup of functional transistors. In studies to date, only the DC characteristics of a gate array MOSFET have been measured after wiring to laser deposited polysilicon lines and probe pads (see figures 2 and 4); operation was consistent with expected device performance.

Acknowledgments

The authors wish to thank Drs. J. Rittmann and D. B. Tuckerman for several valuable technical discussions; D. Duerre, L. R. Mendonca, A. E. Ormsby, W. F. Gee, and W. C. Wilson for expert technical assistance throughout this work; J. Trevino and J. Fischer for assisting with sample preparation and analysis; and Chris Ghinazzi for expert assistance in preparing the manuscript.

Work performed under the auspices of the U.S. Department of Energy by the Lawrence Livermore National Laboratory under Contract W-7405-Eng-48.

References

1. D. J. Ehrlich and J. Y. Taso, "Laser direct writing for VLSI," in *VLSI Electronics: Microstructure Science*, **7**, Einspruch, N. (editor), Academic Press, New york, 1983.
2. R. M. Osgood Jr., "Laser microchemistry and its application to electron-device fabrication," *Ann. Rev. Phys. Chem*, **34**,(1983).
3. I. P. Herman, R. A. Hyde, B. M. McWilliams, A. H. Weisberg and L. L. Wood, Materials Research Society Symposia Proceedings (November 1982), **17**, *Laser Diagnostics and Photochemical Processing Semiconductor Devices*, edited by R. M. Osgood Jr, S. R. J. Brueck and H. R. Schlossberg, (Elsevier, New York, 1983), p. 9.
4. I. P. Herman, B. M. McWilliams, F. Mitlitsky, H. W. Chin, R. A. Hyde, L. L. Wood, Materials Research Society Symposia Proceedings (1983) (to be published).
5. D. Bäuerle, Materials Research Society Symposia Proceedings (November 1982), **17**, *Laser Diagnostics and Photochemical Processing Semiconductor Devices*, edited by R. M. Osgood Jr, S. R. J. Brueck and H. R. Schlossberg, (Elsevier, New York, 1983) p. 19.
6. S. D. Allen, *J. Appl. Phys.*, **52**, 11(Nov. 1981).
7. D. J. Ehrlich, R. M. Osgood Jr., and T. F. Deutsch, *Appl. Phys. Lett.*, **39**, 957(1981).
8. D. Bäuerle, P. Irsigler, G. Leyendecker, H. Noll and D. Wagner, *Appl. Phys. Lett.*, **40**, 819(1982).
9. B. M. McWilliams, I. P. Herman, F. Mitlitsky, R. A. Hyde and L. L. Wood, *Appl. Phys. Lett.*, **43**, 946(1983).
10. S. D. Allen and A. B. Tringubo, *J. Appl. Phys.*, **54**, 3(March 1983).
11. D. J. Ehrlich, R. M. Osgood Jr., and T. F. Deutsch, *Appl. Phys. Lett.*, **36**, 698(1980).
12. J. I. Steinfeld, T. G. Anderson, C. Raiser, D. R. Denison, L. D. Hartsough, and J. R. Hollahan, *J. Electrochem. Soc.*, **127**, 514 (1980).
13. D. J. Chuang, *J. Chem. Phys.*, **72**, 6303(1980).
14. J. E. Moody and R. H. Hendel, *J. Appl. Phys.*, **53**, 4364 (1982).
15. Y. I. Nissim, A. Lietoila, R. B. Gold and J. F. Gibbons, *J. Appl. Phys.*, **51**, 274(1980).
16. M. L. Burgener, R. E. Reedy, *J. Appl. Phys.*, **53**, 4357(1982).
17. J. J. Yang, W. I. Simpson and R. P. Ruth, *J. Electron. Mat.*, **10**, 1011(1981).
18. H. Kurokawa, *J. Electrochem. Soc.*, **129**, 2620(1982).
19. N. Gerzberg and J. Meindl, *IEEE Electron Device Lett.*, **EOL-1**, No. 3, March 1980.

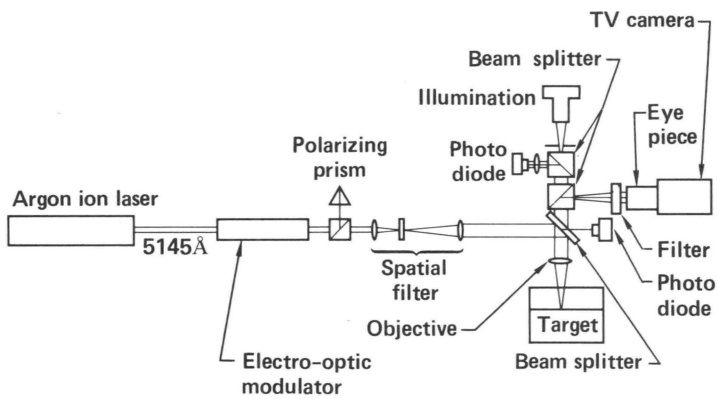

Figure 1. Experimental Apparatus

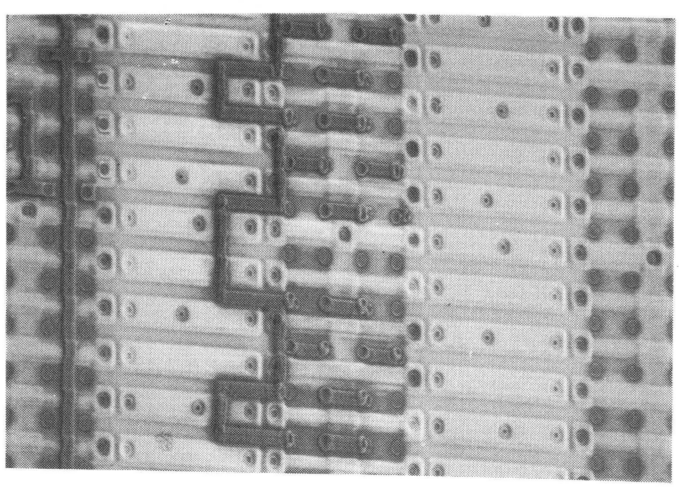

Figure 2. Devices interconnected with laser deposition of doped polysilicon.

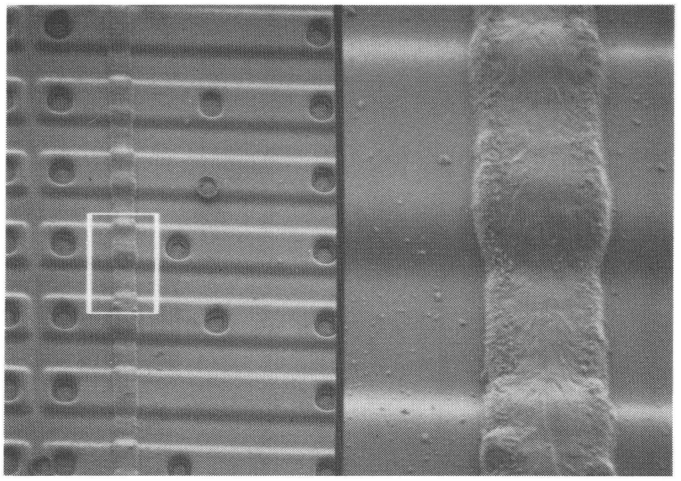

Figure 3. Example of a line used for resistivity measurements.

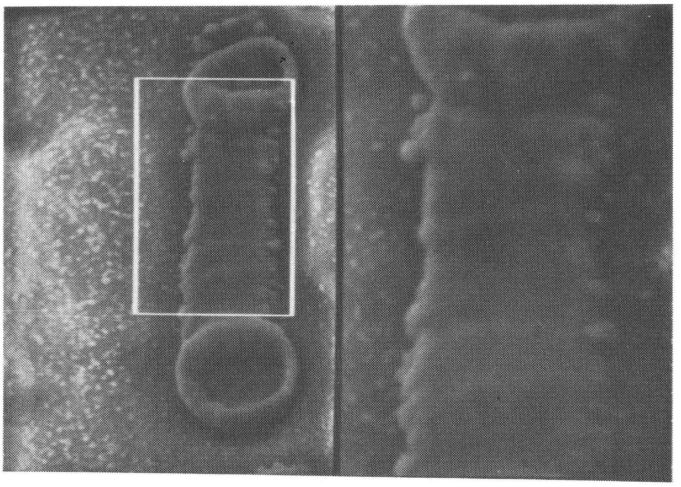

Figure 4. Example of a laser deposited doped polysilicon line contacting device structures.